

# Macula Ganglion Cell Thickness Changes Display Location-Specific Variation Patterns in Intermediate Age-Related Macular Degeneration

Matt Trinh,<sup>1,2</sup> Janelle Tong,<sup>1,2</sup> Nayuta Yoshioka,<sup>1,2</sup> Barbara Zangerl,<sup>1,2</sup> Michael Kalloniatis,<sup>1,2</sup> and Lisa Nivison-Smith<sup>1,2</sup>

<sup>1</sup>Centre for Eye Health, University of New South Wales, Sydney, Australia

<sup>2</sup>School of Optometry and Vision Science, University of New South Wales, Sydney, Australia

Correspondence: Lisa Nivison-Smith, School of Optometry and Vision Science, University of New South Wales, Sydney 2052, New South Wales, Australia; [l.nivison-smith@unsw.edu.au](mailto:l.nivison-smith@unsw.edu.au).

**Received:** October 2, 2019

**Accepted:** November 16, 2019

**Published:** March 9, 2020

Citation: Trinh M, Tong J, Yoshioka N, Zangerl B, Kalloniatis M, Nivison-Smith L. Macula ganglion cell thickness changes display location-specific variation patterns in intermediate age-related macular degeneration. *Invest Ophthalmol Vis Sci*. 2020;61(3):2. <https://doi.org/10.1167/iovs.61.3.2>

**PURPOSE.** The purpose of this study was to examine changes in the ganglion cell layer (GCL) of individuals with intermediate age-related macular degeneration (AMD) using grid-wise analysis for macular optical coherence tomography (OCT) volume scans. We also aim to validate the use of age-correction functions for GCL thickness in diseased eyes.

**METHODS.** OCT macular cube scans covering  $30^\circ \times 25^\circ$  were acquired using Spectralis spectral-domain OCT for 87 eyes with intermediate AMD, 77 age-matched normal eyes, and 254 non-age-matched normal eyes. The thickness of the ganglion cell layer (GCL) was defined after segmentation at 60 locations across an  $8 \times 8$  grid centered on the fovea, where each grid location covered  $0.74 \text{ mm}^2$  (approximately  $3^\circ \times 3^\circ$ ) within the macula. Each GCL location of normal eyes ( $n = 77$ ) were assigned to a specific iso-ganglion cell density cluster in the macula, based on patterns of age-related GCL thickness loss. Analyses were then performed comparing AMD GCL grid-wise data against corresponding spatial clusters, and significant AMD GCL thickness changes were denoted as values outside the 95% distribution limits.

**RESULTS.** Analysis of GCL thickness changes revealed significant differences between spatial clusters, with thinning toward the fovea, and thickening toward the peripheral macula. The direction of GCL thickness changes in AMD were associated more so with thickening than thinning in all analyses. Results were corroborated by the application of GCL thickness age-correction functions.

**CONCLUSIONS.** GCL thickness changed significantly and nonuniformly within the macula of intermediate AMD eyes. Further characterization of these changes is critical to improve diagnoses and monitoring of GCL-altering pathologies.

**Keywords:** optical coherence tomography, age-related macular degeneration, inner retinal thickness

Age-related macular degeneration (AMD) is a leading cause of irreversible blindness in developed countries for people over 60 years of age<sup>1</sup> and is classically characterized by degeneration of the outer retina within the macula. Emerging evidence, however, suggests the inner retina may also be subject to a host of changes secondary to outer retinal degeneration in AMD. Defining the ganglion cell layer (GCL) thickness profile in intermediate AMD eyes is vital, as nonexudative AMD shows increased rates of comorbidity with other GCL thickness altering<sup>2,3</sup> pathologies, such as glaucoma<sup>4</sup> and diabetic retinopathy,<sup>5</sup> potentially obscuring GCL thickness interpretations.

In histological studies, Medeiros and Curcio<sup>6</sup> have demonstrated a 53% loss in ganglion cell number with exudative AMD compared to age-match control eyes. Sullivan and colleagues<sup>7</sup> demonstrated sprouting and extension of rod bipolar cells dendrites in nonexudative AMD eyes. More recently, Jones et al.<sup>8</sup> demonstrated transloca-

tion of amacrine cells, changes in neuronal neurotransmitter profiles, and changes in metabolic profiles of Müller cells in both exudative and nonexudative eyes, particularly in areas above drusen deposits.

In vivo, inner retinal changes have been reported for various stages of AMD as loss of GCL thickness<sup>9</sup>; inner plexiform layer (IPL) thickness<sup>10</sup>; ganglion cell (GC)-IPL thickness<sup>11</sup>; and ganglion cell complex (GCL-IPL and retinal nerve fiber layer [RNFL]) thickness and volume.<sup>9,12-15</sup> These inner retinal changes have been associated with poor photoreceptor integrity<sup>12</sup> and retinal vascular alterations.<sup>16-18</sup> Alterations in pupil response in advanced AMD suggest remaining inner retinal neurons in AMD, such as melanopsin ganglion cells, may also be dysfunctional.<sup>19</sup>

Previous studies' in vivo quantification of inner retinal changes in AMD have been relatively constrained by two problems. First, due to limited analytical tools, GCL thickness measurements have been measured either globally or

through arbitrarily-defined parameters with tenuous structural and functional basis.<sup>9,11–15,20,21</sup> Thus, it is not known if inner retinal changes in AMD exhibit a specific spatial distribution. This is relevant considering functional testing and postmortem analysis of photoreceptor distribution suggest the parafovea to be particularly susceptible to outer retinal degeneration in AMD.<sup>22,23</sup> Second, limitations may also arise in establishing age and sex-matched cohorts in studies, particularly with regard to diseases such as AMD, which tend to have a predilection for older women.<sup>24</sup> The use of age-correction functions to account for heterogeneous and under-sampled cohorts has been previously demonstrated for visual field data,<sup>25</sup> and recently described age-correction functions for GCL thickness changes across the macula may have potential to do the same.<sup>26</sup>

Our group has recently described methodology to quantify GCL thickness changes across the macula with high spatial resolution using spectral domain optical coherence tomography (SD-OCT)<sup>26,27</sup> and age-correction functions for GCL thickness across the macula. The former methodology has successfully been used to describe rates of age-related GCL thickness loss in specific areas of the macula,<sup>26,27</sup> illustrate contrast sensitivity isocontours of visual field to better delineate functional deficits,<sup>28,29</sup> and develop accurate spatial modeling of visual field isocontours allowing for better assessment of glaucoma progression.<sup>30</sup> Thus, this study will investigate the spatial distribution of inner retinal changes in eyes with AMD using high spatial resolution SD-OCT techniques based on previously described clustering methods.<sup>26,27</sup> We also aim to validate the use of newly developed age-correction functions<sup>26</sup> for GCL thickness in both normal populations and in AMD.

## MATERIALS AND METHODS

### Study Population

All patient data were obtained through retrospective analysis of records from July 12, 2010, to February 28, 2017, of patients attending the Centre for Eye Health (CFEH) Sydney, Australia. CFEH is a referral-only clinic providing advanced diagnostic eye testing by specially trained optometrists and ophthalmologists.<sup>31</sup> All patients had given prior written consent to use their data for research in accordance with the Declaration of Helsinki and approved by the Biomedical Human Research Ethics Advisory Panel of the University of New South Wales.

Inclusion criteria for normal eyes were no evidence of ocular disease, including but not limited to glaucoma, diabetic retinopathy, AMD, or signs of subretinal or intraretinal deposits, fluid, pigment, or vascular changes at the macula.<sup>32</sup> Normal eyes were then assigned to one of two groups—age-matched normal eyes ( $n = 77$ ) or non-age-matched normal eyes ( $n = 254$ ). Inclusion criteria for eyes with AMD were age of 50 years or older, diagnosis of intermediate AMD,<sup>33</sup> and no evidence of late AMD signs, such as neovascularization and/or geographic atrophy. Classification of AMD was based on evaluation of fundus photography, scanning laser ophthalmoscopy photography, and optical coherence tomography (OCT) between at least two nonblind investigators using the Ferris classification system.<sup>33</sup> Specifically, intermediate eyes comprised of large drusen ( $>125 \mu\text{m}$ ) or pigmentary abnormalities associated with at least medium drusen ( $63\text{--}125 \mu\text{m}$ ).

### Image Acquisition

OCT macular cube scans (61 B-scans covering an area of  $30^\circ \times 25^\circ$ ) were acquired with Spectralis SD-OCT (Heidelberg Engineering, Heidelberg, Germany), as previously described.<sup>26,27</sup> Scans with significant artifacts or signal strength of lower than 15 dB were excluded. Scans were automatically segmented into each individual retinal layer using the HRA/Spectralis Viewing Module (Heidelberg Engineering). The GCL was reviewed (Fig. 1A) in all scans and manually corrected if necessary. GCL thickness was then extracted from across the macula as 64 measurements within an  $8 \times 8$  grid centered on the fovea (each grid location covering  $0.74 \text{ mm}^2$  [approximately  $3^\circ \times 3^\circ$ ]; Fig. 1B). For scans where manual correction was not possible, grid locations were excluded from the analysis. If an eye had  $>10\%$  of grid locations missing, the eye was excluded from the analysis.<sup>27</sup>

### Normative Data and Spatial Clusters

Our previous work has established that grid locations across the macula in normal healthy eyes can be assigned to specific spatial clusters based on statistically isometric patterns of an age-related GCL thickness profile.<sup>26,27</sup> These spatial clusters are robust, manifested through a variety of clustering techniques, including hierarchical, k-means, and pattern recognition methods. Although several cluster patterns were previously described, we applied the pattern resulting in the greatest structure-function concordance in 5-year average normative data to the current study (Fig. 1C).<sup>26</sup> Subsequently, normative data for this study were generated by grouping eyes of normal participants into 5-year age brackets of 50 to 54, 55 to 59, 60 to 64, 65 to 69, 70 to 74, 75 to 79, and 80+ years old. Average GCL thickness for each grid location was then pooled to calculate the mean cluster GCL thickness for each age-bracket (Fig. 2A). To maintain consistency when comparing clustered data, the fovea area corresponding to the central four grids were excluded from the analysis due to its significantly variable ganglion cell density.<sup>34</sup> Thus, the total number of grids analyzed was 60 for each eye.

### Age-Matched GCL Thickness Analysis of AMD Eyes

For each AMD eye, GCL thickness of each grid location was compared to the normative mean of the corresponding spatial cluster for their relevant age-matched bracket. Thickness measurements outside the 95% distribution limits (i.e., outside two SDs) of the relevant age-matched normal grid location were flagged and categorized as significant GCL thickening (top 2.5% of values) or thinning (bottom 2.5% of values). The magnitude of GCL change for each location within AMD eyes was expressed as the number of SDs away from the normal cluster mean, to account for the varying thickness across the macula.<sup>34</sup>

The direction of change across all AMD eyes was then described by the additive GCL thickness change, where the number of SDs from normal was averaged across all flagged locations in all AMD eyes. A positive additive GCL thickness value suggests overall GCL thickening across AMD eyes, whereas a negative value suggests overall GCL thinning.

The magnitude of GCL change across all AMD eyes was described by the absolute GCL thickness change, where the number of SDs from normal were converted to absolute

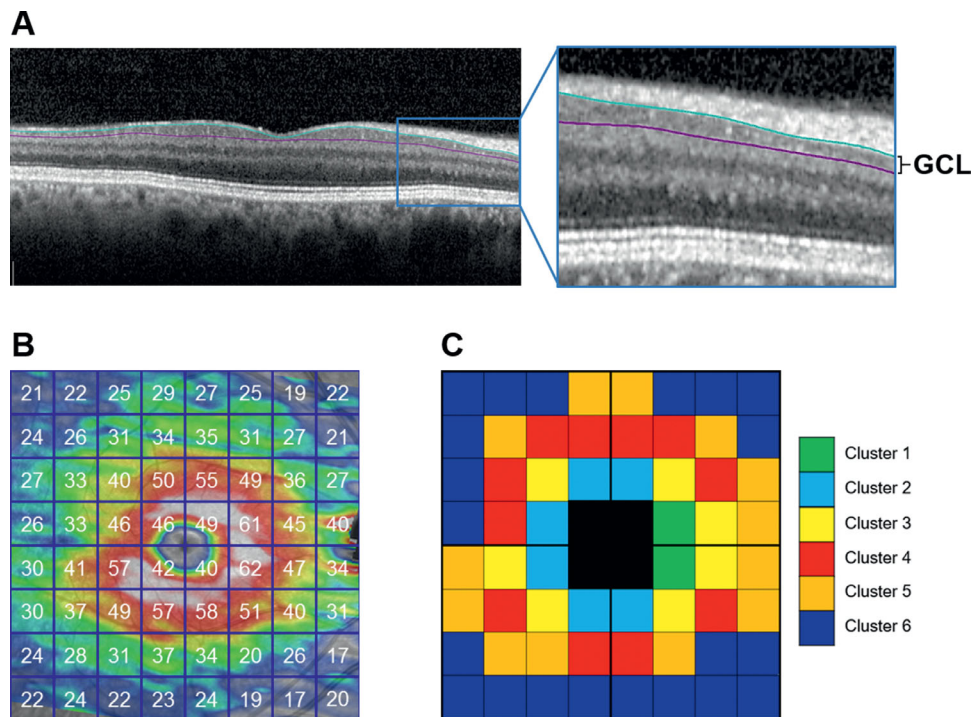


**FIGURE 1.** (A) GCL segmented within the HRA/Spectralis Viewing Module – manual correction was performed when necessary, and (B) Spectralis  $8 \times 8$  grid centred on the fovea, each grid location covering  $0.74 \text{ mm}^2$  (approximately  $3^\circ \times 3^\circ$ ). Values indicate the average GCL thickness for that location in micrometers. (C) Iso-ganglion cell density spatial clusters pattern used in this study, based on Tong et al.<sup>26</sup>; the  $8 \times 8$  grids totaled  $6880 \mu\text{m} \times 6880 \mu\text{m}$ , centered on the fovea with each grid occupying  $0.74 \text{ mm}^2$ . The foveal area corresponding to the central four grids were excluded from the analysis, due to variable ganglion cell density.<sup>54</sup>

**TABLE 1.** Tong et al.'s<sup>26</sup> GCL Thickness Functions' Regression Coefficients

Cluster	a	b
1	-0.0032	0.25
2	-0.0032	0.25
3	-0.0032	0.25
4	-0.0032	0.25
5	-0.0018	0.13
6	-0.0011	0.08

a, quadratic regression coefficient; b, linear regression coefficient; c, values which were derived individually for each eye's GCL thickness, in microns.

$$Y = ax^2 + bx + c \text{ where } x \text{ is age, and } y \text{ is GCL thickness.}$$

integers (i.e., so that locations exhibiting GCL thinning would no longer represent a negative value) and then averaged.

### Age-Corrected GCL Thickness Analysis

Age-corrected analysis was performed based on GCL functions expressed as location-specific quadratic models (Table 1).<sup>26,27,35</sup> These functions describe GCL thickness change with age in normal eyes, allowing GCL thickness of any macula grid location to be corrected to any age. Hypothetically, these functions enable compensation for cases where distribution of ages in normal cohorts is heterogeneous, by allowing normative GCL thickness data to be age-corrected and then pooled into the desired age category. To validate that these age-correction functions could (1) be used

to compensate for non-age-matched normative data populations, and (2) be applied beyond normal eyes to age-correct diseased eyes as well, functions were used to correct GCL thickness data of all normal eyes, AMD eyes, and a non-age-matched normal cohort ( $n = 254$ ) to the equivalent of a 65-year-old eye.<sup>26</sup> Analyses were then repeated as in age-matched analyses, where locations in AMD eyes were flagged as exhibiting significant GCL thickening or thinning if the magnitude of GCL change was greater than 2 SDs from the normal cluster mean.

Further comparisons were performed with the normal<sub>non-age-matched</sub> cohort, in order to corroborate age-correction functions for GCL thickness. Thus, there were two age-corrected analyses: "age-corrected," which used the age-matched, normal population ( $n = 77$ ) for age-correction; and "age-corrected<sub>non-age-matched</sub>," which used the heterogeneously age-distributed normal population ( $n = 254$ ) for age-correction (Table 2).

### Statistical Analysis

Statistical analysis for categorical factors between populations was assessed using the  $\chi^2$  test and Fisher's exact test, and between continuous measurements with the Mann-Whitney  $U$ -test. Assessment of GCL thickness change between subpopulations and spatial locations was assessed by a Kruskal-Wallis test with post hoc Dunn's multiple comparisons test or multiple unpaired  $t$ -test where appropriate. All tests were performed in GraphPad Prism (version 8; GraphPad Software, Inc., La Jolla, CA, USA) with significance considered as  $P < 0.05$ .

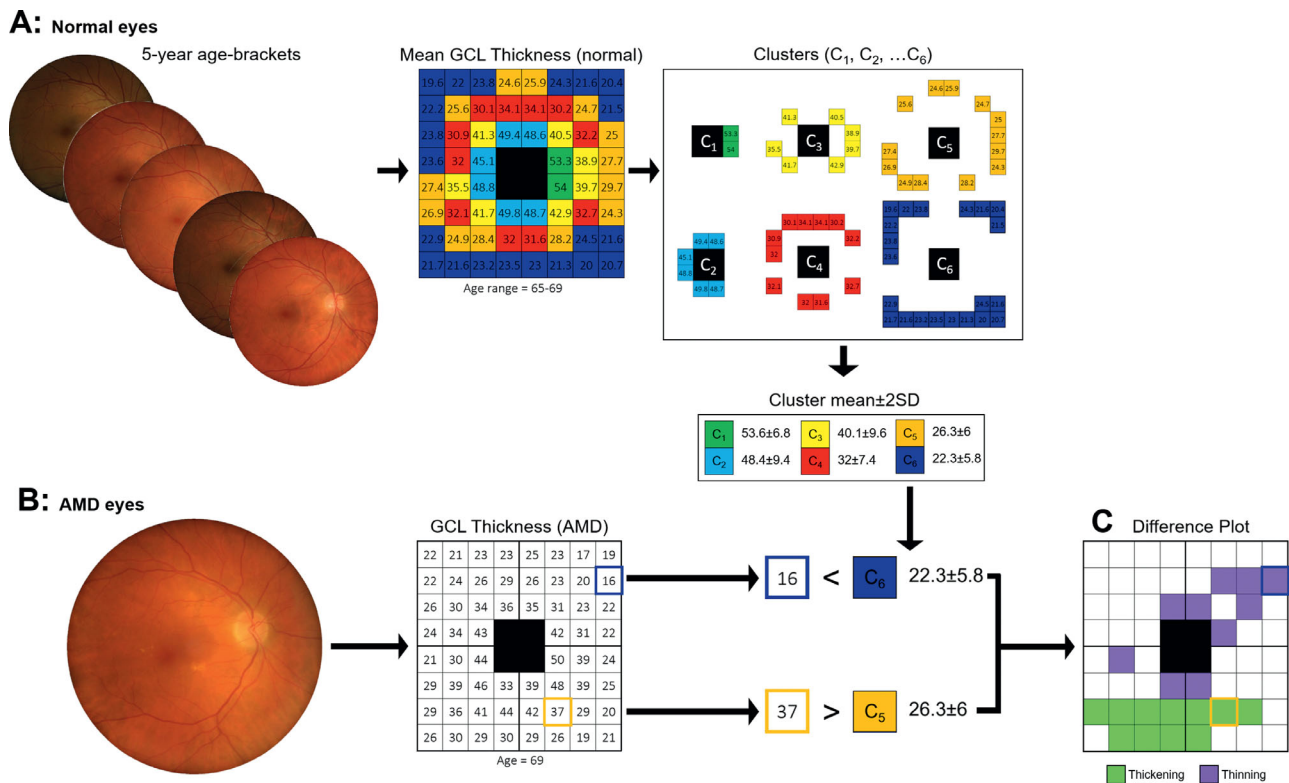


**FIGURE 2.** Example of an age-matched analysis for an eye of a 69-year-old Caucasian woman with intermediate AMD. (A) Mean GCL thickness of all normal eyes' grid locations in the corresponding 5-year age bracket. Grid locations were separated into spatial clusters, which show statistically isometric GCL thickness values,<sup>21</sup> and then the mean ± 2 SDs of each cluster was calculated. The four central grid locations were excluded due to high variability of GCL measurements at the fovea. (B) GCL thickness of each grid location in AMD eyes. (C) Each grid location of AMD eyes were then compared to the corresponding spatial cluster as determined in A, and a difference plot was created from values outside the mean ± 2 SDs of normal eyes. Examples of other difference plots are provided.

**RESULTS**

**Subject Demographics**

Seventy-seven normal eyes from 77 age-matched participants and 87 eyes from 87 participants with intermediate AMD were included in the study. There was no significant difference with age and gender between the two groups. There was significant difference in best-corrected visual acuity (BCVA) and refractive error between the normal and AMD cohort, with AMD participants more likely to have poorer BCVA and a greater hypermetropic refractive error (Table 2). However, the mean refractive error values were relatively low and, hence, it was expected that this, along with axial length, would not significantly impact results. For validation of age-correction functions, an additional non-age-matched normative population consisting of 254 eyes from 254 normal participants was also included. As expected, this population demonstrated a significantly different distribution of ages compared to the normal and intermediate AMD cohorts ( $\chi^2$  test;  $P < 0.0001$ ).

**GCL Thickness Change in AMD Eyes Based on Age-Matched Analysis**

Normal cohort data were processed to generate normative mean GCL thickness of each spatial cluster.<sup>26,27</sup> The mean GCL thickness for each cluster for each 5-year age-bracket is described in Table 3.

Individual locations for each AMD eye were then compared to its relevant cluster mean (Figs. 2A, 2B). When each AMD eye was inspected individually, a variety of configurations of GCL thickness changes, including thickening and/or thinning, were observed (Fig. 2C). The magnitude of GCL thickness change for each flagged location also seemed to vary within individual AMD eyes, with some locations demonstrating thickness changes over 10 SDs away from the normative mean (Fig. 3A). Interestingly, there was a significant correlation between the increasing number of locations flagged and a greater magnitude of GCL thickness change (Spearman's  $r = 0.37$ ;  $P < 0.01$ ; Fig. 3B). No ocular or demographic factors were found to be significantly correlated with the number of locations flagged, including age ( $P = 0.28$ ).

When the AMD cohort was assessed as a whole, 83.9% (73/87) of AMD eyes had at least one grid location (0.74 mm<sup>2</sup>, approximately 3° × 3°) flagged as exhibiting significant GCL thickening or thinning versus an age-matched, normative group. Overall, the mean number of locations flagged in AMD eyes were 3.2, corresponding to a mean GCL thickness change spanning across 2.22 mm<sup>2</sup>, approximately 9.6° × 9.6° within the macula. Forty-one percent (36/87) of AMD eyes had locations flagged that exhibited significant GCL thickening only, 23% (20/87) had locations flagged that exhibited significant GCL thinning only, and 18.4% (16/87) had locations flagged that exhibited both significant GCL thickening and thinning.

In regard to the direction of change for the whole AMD cohort, the additive mean GCL thickness change from

TABLE 2. Subject Demographics

	Normal	Intermediate AMD	P Value	Normal <sub>non-age-matched</sub>
Eyes, <i>n</i>	77	87		254
Age, y				
Mean	66	69		50
Range	50–85	51–89		20–85
20–49	0	0		124
50–54	5	3		34
55–59	11	9		32
60–64	23	14		26
65–69	14	21	0.11*	14
70–74	12	21		12
75–79	6	15		6
80+	6	4		6
Sex				
Males	36 (46.8%)	30 (34.5%)	0.11†	109
Females	41 (53.2%)	57 (65.5%)		145
BCVA (logMAR)				
Mean	0.01	0.06	< 0.01‡	0.06
Range	–0.1 to –0.2	–0.08 to –0.4		–0.3 to –2.2
Refractive error (D)				
Mean	+0.22	+1.15	< 0.01‡	–0.48
Range	–5.38 to +3.75	–2.75 to +6.00		–6.00 to +3.00

\* Chi-square test.

† Fisher's exact test.

‡ Mann–Whitney *U* test.TABLE 3. Normal GCL Thickness Mean  $\pm$  2 SD ( $\mu$ m) for Each Cluster Per 5-year Age Bracket

Age	C <sub>1</sub>	C <sub>2</sub>	C <sub>3</sub>	C <sub>4</sub>	C <sub>5</sub>	C <sub>6</sub>
50–54	55.7 $\pm$ 4.2	50.9 $\pm$ 6.4	41.8 $\pm$ 8	33.3 $\pm$ 6.2	28 $\pm$ 6.4	23 $\pm$ 6
55–59	58 $\pm$ 10.2	52.2 $\pm$ 12	43.2 $\pm$ 11	33.6 $\pm$ 9.6	26.9 $\pm$ 7.2	22.2 $\pm$ 6
60–64	55.4 $\pm$ 8.8	50.9 $\pm$ 9.8	42.1 $\pm$ 10.4	33.4 $\pm$ 8.4	27.3 $\pm$ 6.4	22.8 $\pm$ 5.6
65–69	53.6 $\pm$ 6.8	48.4 $\pm$ 9.4	40.1 $\pm$ 9.6	32 $\pm$ 7.4	26.3 $\pm$ 6	22.3 $\pm$ 5.8
70–74	50.5 $\pm$ 10.4	48.9 $\pm$ 9.4	38.5 $\pm$ 10.2	31 $\pm$ 8.6	25.5 $\pm$ 6.4	22 $\pm$ 5.8
75–79	48.6 $\pm$ 14.2	46 $\pm$ 13	37.7 $\pm$ 11.8	30.2 $\pm$ 9.4	25.3 $\pm$ 5.8	21.3 $\pm$ 5
80+	47.3 $\pm$ 10.2	44.8 $\pm$ 10.2	37.6 $\pm$ 8.6	30.2 $\pm$ 6.4	25.1 $\pm$ 5.4	21.4 $\pm$ 5.6
65 (corrected)	54 $\pm$ 9.8	49.9 $\pm$ 10.2	41 $\pm$ 10.2	32.7 $\pm$ 8.2	26.7 $\pm$ 6.4	22.4 $\pm$ 5.6

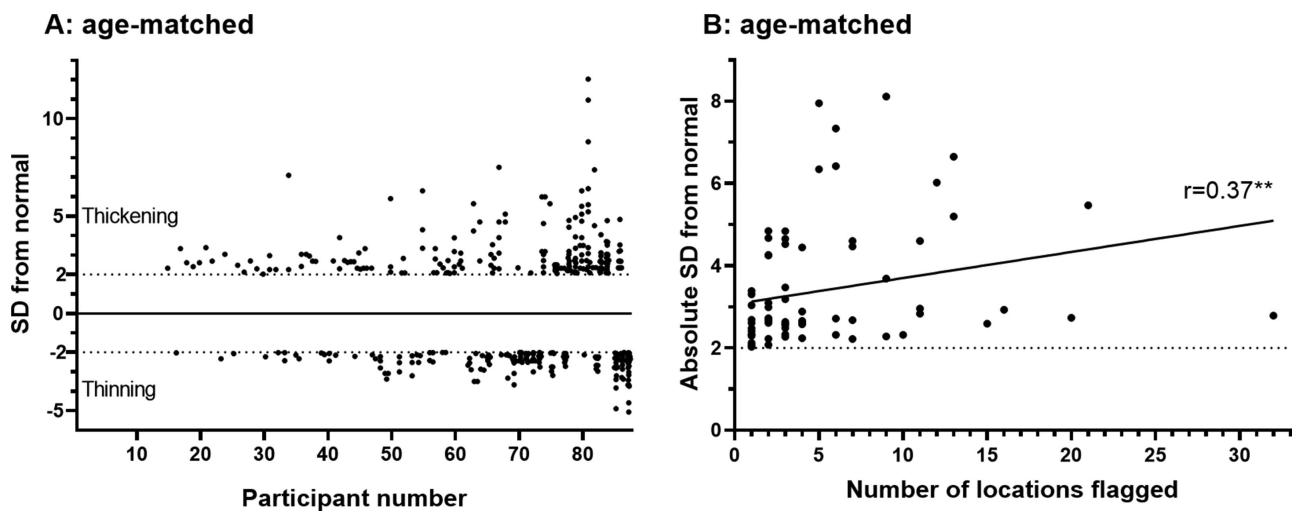
C<sub>1</sub> to C<sub>6</sub>, cluster 1 to cluster 6.

FIGURE 3. (A) Plot of all grid locations for all 87 AMD eyes, which were flagged as significantly different, based on GCL thickness being more than 2 SDs from the age-matched mean GCL thickness of normal eyes at the corresponding spatial cluster. Eyes were arranged in order of increasing frequency of grid locations flagged, so that participants 1 to 14 have no data points as they had no locations with significant GCL thickness change. Y-axis indicates the magnitude of SDs from the normal mean. (B) Correlation between the number of grid locations flagged versus the absolute SD from normal based on age-matched data for all flagged locations in that eye (absolute mean SD from normal = mean SD of thickening locations + |mean SD of thinning locations|). \*\* =  $P < 0.01$ .

TABLE 4. Comparisons of Age-Matched Versus Age-Corrected Versus Age-Corrected<sub>non-age-matched</sub> Analyses

	Age-Matched	Age-Corrected	Age-Corrected <sub>non-age-matched</sub>	P Value
AMD eyes with GCL thickness change	73/87 (83.9%)	74/87 (85.1%)	78/87 (89.7%)	0.53*
Thickening only	36/87 (41.4%)	41/87 (47.1%)	39/87 (44.8%)	
Thinning only	20/87 (23%)	19/87 (21.8%)	21/87 (24.1%)	0.95†
Thickening and thinning	16/87 (18.4%)	14/87 (16.1%)	18/87 (20.7%)	
Mean total change (additive)±SD [SD]	0.44±3.05	0.56±2.97	0.29±2.98	0.28*
Mean thickening	3.17±1.47	3.11±1.44	3.07±1.37	0.67*
Mean thinning	-2.51±0.53	-2.42±0.41	-2.51±0.48	0.19*
Total grid locations with GCL thickness change	381/5220 (7.3%)	353/5220 (6.8%)	428/5220 (8.2%)	0.43*
Thickening	198/5220 (3.8%)	190/5220 (3.6%)	215/5220 (4.1%)	0.61†
Thinning	183/5220 (3.5%)	163/5220 (3.1%)	213/5220 (4.1%)	
Flagged grid locations concurrent in all analyses	309/5220 (5.9%)	309/5220 (5.9%)	309/5220 (5.9%)	
Thickening	179/5220 (3.4%)	179/5220 (3.4%)	179/5220 (3.4%)	
Thinning	130/5220 (2.5%)	130/5220 (2.5%)	130/5220 (2.5%)	
Thickening mean±SD	3.31±1.4	3.19±1.35	3.27±1.32	0.25*
Thinning mean	-2.7±0.59	-2.65±0.46	-2.77±0.52	0.17*
Flagged grid locations exclusive to each analysis	47/5220 (0.9%)	0/5220 (0%)	50/5220 (1%)	0.29‡
Thickening	17/5220 (0.3%)	0/5220 (0%)	23/5220 (0.4%)	0.33†
Thinning	30/5220 (0.6%)	0/5220 (0%)	27/5220 (0.5%)	
Thickening mean±SD	2.48±0.22	—	2.47±0.29	0.34‡
Thinning mean	-2.33±0.23	—	-2.34±0.26	0.81‡

\* Kruskal–Wallis test.

† Chi-square test.

‡ Mann–Whitney *U* test.

normal was positive ( $0.44 \pm 3.05$ ), suggesting a trend toward GCL thickening rather than thinning in AMD eyes overall (Table 4). This trend, in part, may have been due to a larger number of the total 5220 possible grid locations exhibiting GCL thickening than thinning, although this difference did not reach statistical significance (3.8% [198/5220] locations exhibiting thickening vs. 3.5% [183/5220] exhibiting thinning;  $P = 0.09$ ). This direction of change may also have been due to the mean SD of locations exhibiting GCL thickening having a greater magnitude of change than locations exhibiting GCL thinning ( $3.17 \pm 1.47$  vs.  $-2.51 \pm 0.53$ );  $P < 0.0001$ ).

### Spatial Distribution of GCL Thickness Change

The spatial distribution of GCL thickness change in AMD eyes was then assessed to determine if specific areas of the macula were more susceptible to change than others. Flagged locations were assigned to the relevant spatial cluster (Fig. 1C) and the magnitude and direction of GCL thickness changes were assessed between and within each cluster.

In regard to the direction of change, the additive mean GCL thickness change from normal showed significant difference between clusters (Kruskal–Wallis test  $P < 0.0001$ ). Post hoc analysis (Dunn's multiple comparisons test) showed this change to be negative for clusters toward the fovea (clusters 1–3) suggesting a trend toward GCL thinning, and positive for clusters toward the periphery (clusters 5 and 6) suggesting GCL thickening. These results suggest an eccentricity dependent effect in GCL thickness for AMD eyes (Fig. 4A).

Clusters were further assessed by magnitude, by separating locations of GCL thickening from thinning within each cluster. The absolute mean GCL thickness change from normal showed significant difference between clusters (Kruskal–Wallis test  $P < 0.001$ ; Fig. 4B), and post hoc analysis (Dunn's multiple comparisons test) showed a greater magnitude of GCL thickening in cluster six compared to four ( $P < 0.01$ ; Fig. 4B), but no significant difference with regard to the magnitudes of GCL thinning. Within each cluster, GCL change was significantly greater for locations exhibiting thickening compared to thinning in the outer clusters (i.e., clusters 5 and 6;  $P < 0.01$  both). Other clusters did not show a significant difference when comparing the magnitudes of GCL thickening and thinning.

### GCL Thickness Change in AMD Eyes Based on Age-Corrected Analyses

Finally, we assessed whether GCL thickness changes in AMD eyes could also be observed using a recently described methodology for age-correction of GCL thickness across all grid locations in the macula.<sup>26</sup> We hypothesized that use of age-correction would allow for GCL thickness changes in AMD eyes to be observed when compared against an age-matched and a non-age-matched normative population, as all eyes could be corrected to a single desired age bracket. To confirm this, location-specific conversion equations (Table 1) were used to correct GCL thickness for all normal eyes, AMD eyes, and an additional normal<sub>non-age-matched</sub> population (comprised of 254 heterogeneously age-distributed participants' eyes) to the equivalent of 65-year-old eyes. Each grid

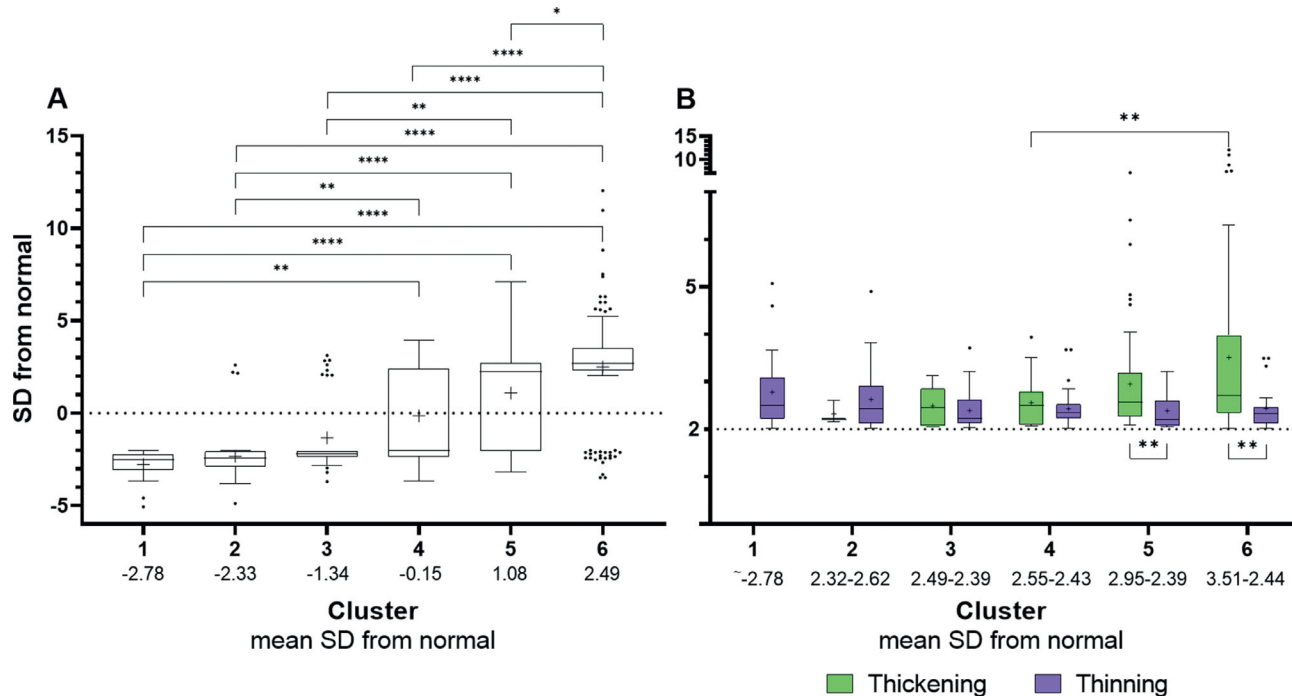


**FIGURE 4.** (A) Additive mean SD from normal for each cluster (GCL thickening + GCL thinning), displayed as box and whisker plots via the Tukey method (whiskers extend to  $1.5 \times$  interquartile range and values exceeding this are plotted as individual points). + = Indicates mean (thickening and thinning values provided beneath X-axis); significance  $P$  values denoted by: \* =  $P < 0.05$ , \*\* =  $P < 0.01$ , \*\*\*\* =  $P < 0.0001$ . (B) Absolute mean SD from normal for each cluster (separated into thickening and thinning), displayed as box and whisker plots via the Tukey method as described in B. ~ = no values were flagged for thickening in cluster 1.

location for all AMD eyes was then again compared to its corresponding cluster's normative mean, for both normal cohorts.

As with the age-matched analysis, there was significant variation in the number of flagged locations and the magnitude of GCL thickness change among individual age-corrected AMD eyes when compared to either normative cohort (Figs. 5A, 5C). A significant correlation between the increasing number of locations flagged and a greater magnitude GCL thickness change also remained following age-correction, with both the normal and normal<sub>non-age-matched</sub> cohorts (Spearman's  $r = 0.52$ ;  $P < 0.0001$ ; Figs. 5B, 5D).

Age-matched, age-corrected, and age-corrected<sub>non-age-matched</sub> analyses were then compared directly to each other. There was no statistically significant difference in the distribution of eyes with flagged locations ( $\chi^2$  test,  $P = 0.95$ ), or in the magnitude or proportion of locations exhibiting total, thickening, or thinning GCL changes (Table 4). Furthermore, no significant differences were found between the age-matched and age-corrected correlations (Figs. 2B; 5B, 5D) between the number of grid locations flagged versus the absolute SD from normal (z-test,  $P > 0.25$  for all comparisons).

The congruency of locations that were flagged by each analysis was also compared. We found that of all the locations flagged in age-matched (381/5220), age-corrected (353/5220), and age-corrected<sub>non-age-matched</sub> (428/5220) analyses, the majority were concurrently flagged (309/5220; 81%, 88%, and 72%, respectively). These concurrently flagged locations more commonly exhibited GCL thickening than thinning, and also exhibited a greater magnitude of GCL thickness change (Table 4; Fig. 6A). Overall, there was no statistically significant difference between analyses with

regard to the magnitudes of GCL thickening or thinning ( $\chi^2$  test,  $P = 0.25$  and  $0.17$ , respectively) in concurrently flagged locations. Of those not concurrently flagged (i.e., locations flagged exclusive to each analysis), only age-matched and age-corrected<sub>non-age-matched</sub> exhibited such locations (Fig. 6B). There was no statistically significant difference in the proportion of grid locations flagged ( $\chi^2$  test,  $P = 0.33$ ), or magnitude of GCL thickening or thinning (Mann-Whitney  $U$  test,  $P = 0.34$  and  $0.81$ , respectively) for locations exclusive to each analysis.

## DISCUSSION

This study found that significant changes in GCL thickness could be detected within the macula of intermediate AMD eyes using a grid-based analysis. This change varied in direction and magnitude among individual AMD eyes. Overall, however, there was a common spatial distribution of change, with a tendency for GCL thinning toward the fovea and GCL thickening toward the periphery in AMD eyes. GCL thickness changes in AMD eyes were also detected using a non-age-matched normative population and previously derived functions, which allowed for correction of GCL thickness to any age. This suggests that changes in the GCL occur in the early stages of AMD and can be detected with a heterogeneous normative population.

### The Majority of AMD Eyes Exhibit Significant GCL Changes

In this study, we found an average of three locations exhibited significant change in GCL thickness in the macula of

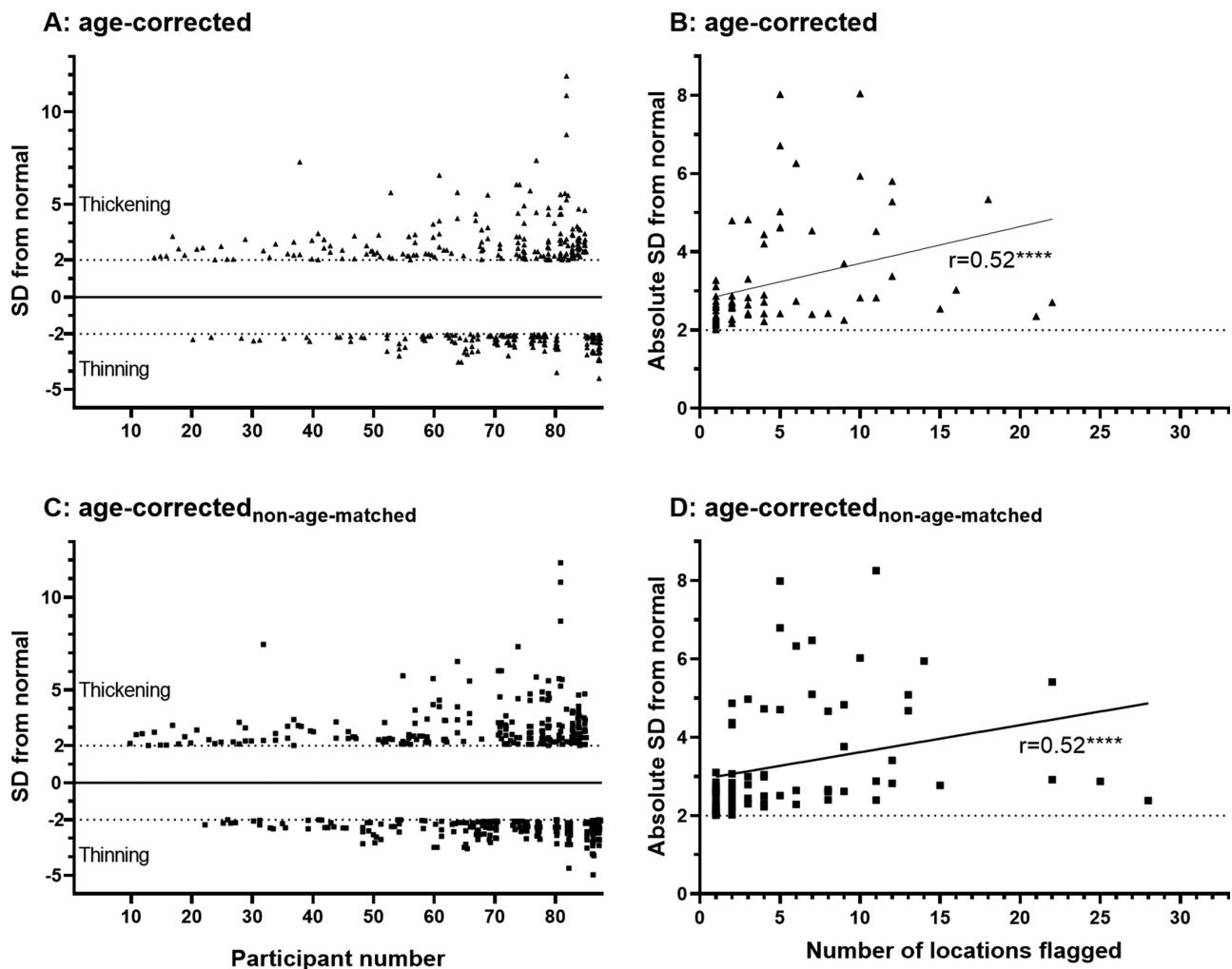


**FIGURE 5.** (A) Plot of all grid locations for all 87 AMD eyes, which were flagged as significantly different, based on age-corrected mean GCL thickness to 65-year-olds. (B) Correlation between the number of grid locations flagged versus the absolute SD from normal based on age-corrected data for all flagged locations in that eye. \*\*\*\* =  $P < 0.0001$ . (C) Plot of all grid locations for all 87 AMD eyes which were flagged as significantly different, based on age-corrected<sub>non-age-matched</sub> mean GCL thickness to 65-year-olds. (D) Correlation between the number of grid locations flagged versus the absolute SD from normal based on age-corrected<sub>non-age-matched</sub> data for all flagged locations in that eye.

AMD eyes, equivalent to an area of approximately  $9.6^\circ \times 9.6^\circ$ . Other studies have shown changes in GCL thickness within a smaller macula area and with less dense spatial sampling.<sup>9,11–15,20,21</sup>

Both GCL thinning and thickening were observed in AMD eyes, with the latter more common. In support of our findings, GCL thickening has been reported recently by Brandl et al.<sup>21</sup> in mild-early AMD (Three Continent AMD Consortium classification).<sup>36</sup> This work, however, was constrained to a 70+ year old cohort, limiting extrapolation of results to a younger population. Our work demonstrates that GCL thickening and thinning also occurs in AMD eyes of a 50+ year old cohort of intermediate AMD eyes. Of other previous literature, most actually contrast our work and Brandl's, suggesting GCL thinning to be more common in nonexudative AMD. The majority of these studies, however, have only implied GCL thinning as a component of the GCL-IPL complex thinning,<sup>11–15,20</sup> and have a number of other limitations, including small sample sizes,<sup>11–15</sup> a lack of age-matching,<sup>12,13,15</sup> auto-segmentation,<sup>11–15,20</sup> which has shown poorer variability compared to manual correction,<sup>37</sup> and less specific spatial

analyses.<sup>13,20</sup> Our study accounted for these limitations by including a large sample size with age-matching, manual correction of segmentation when required, and a location-specific methodology using grid analysis alongside macula spatial clusters, which have proven robust structure-function concordance.<sup>26</sup> These spatial clusters also enabled averaging of the normative data over multiple locations to improve statistical power.

### Proposed Mechanisms for GCL Changes

From the aforementioned studies, mechanisms for GCL thinning in nonexudative AMD include: postreceptor trans-synaptic degeneration<sup>6,10–12,14,20,38</sup>; inner retinal ischaemia<sup>6,10–12,14,16,20</sup>; and mechanical tension from drusen.<sup>12,14,20</sup> Postreceptor trans-synaptic degeneration has been reinforced by strong correlations between the ganglion cell complex and ellipsoid zone reflectivity in AMD subjects but not healthy subjects, suggesting a pathologic dysregulation in the AMD group.<sup>12</sup> The inner retinal ischemia hypothesis has also been supported by demonstration of

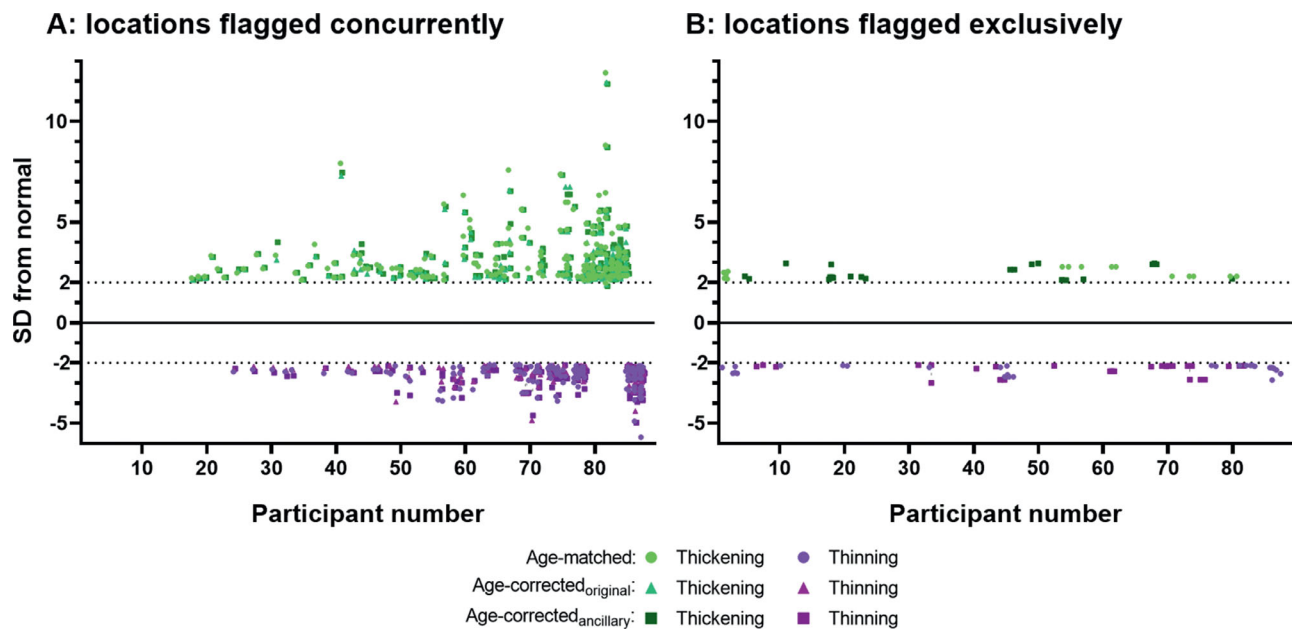


**FIGURE 6.** Congruency of age-corrected and age-matched analyses. (A) Plot of all grid locations that were flagged concurrently in age-matched, age-corrected, and age-corrected<sub>non-age-matched</sub> analyses. ● = indicates data from age-matched analysis; ▲ = indicates data from age-corrected<sub>original</sub> analysis; ■ = indicates data from age-corrected<sub>ancillary</sub> analysis. (B) Plot of all grid locations that were flagged exclusively in only age-matched, age-matched, or age-matched<sub>non-age-matched</sub> analyses.

inner retinal vascular changes in non-neovascular AMD.<sup>16,18</sup> The mechanical tension from drusen proposal, however, has been debated as Borrelli et al. found no relationship between the ganglion cell complex and drusen area or volume.<sup>12</sup> The possibility of drusen regression,<sup>39</sup> however, may complicate these findings.

Proposed mechanisms for GCL thickening in nonexudative AMD include: compensatory proliferation and migration of inter-neuronal cells,<sup>14,40</sup> and reactions to the inflammatory processes in AMD.<sup>41,42</sup> Increased GCL thickness may reflect glial cell hypertrophy and/or neuron migration in the inner retina, events common in other photoreceptor degenerations, such as retinitis pigmentosa.<sup>40</sup> This is supported by recent work of Jones et al.<sup>8</sup> who demonstrated translocation of amacrine cells and changes in Müller cell metabolomics in postmortem advanced AMD eyes. Müller cell changes have also been shown to precede photoreceptor degeneration spatially and temporally in a rat model of AMD, intimating that they could occur in the early and intermediate stages of disease.<sup>43</sup> Alternatively, several studies have shown significant thickening of the inner retina in response to ocular inflammatory events associated with outer retinal thinning.<sup>41,42,44</sup> Inner retinal thickening associated with outer retinal thinning has also been demonstrated in non-exudative AMD eyes.<sup>45</sup> Thus, inner retinal thickening seen in this study could represent the inflammatory component of AMD,<sup>46</sup> although translation of inflammatory physiological changes between different ocular diseases is not certain.

Note, in our study, almost 20% of AMD eyes showed evidence of concurrent GCL thickening and thinning within the macula. Concurrent thickening and thinning has also been shown in intermediate AMD eyes in the outer nuclear layer.<sup>47</sup> These results suggest that the processes leading to thickening and/or thinning are not mutually exclusive, and likely represent components along the same pathophysiological spectrum of AMD progression. This phenomenon is

also important to consider in a clinical context, as GCL thickening and thinning in AMD eyes may mask or exaggerate GCL thinning from other comorbid ocular diseases, such as glaucoma and diabetic retinopathy.<sup>2,3,4,5</sup> As such, the use of local assessment of GCL thickness, as done in this study, may be more effective than summary data for the improved diagnoses and monitoring of GCL-altering pathologies in clinical practice.

### GCL Changes in AMD Demonstrate Specific Spatial Distribution

We found that GCL thickness changes in AMD eyes demonstrated a unique spatial distribution, whereby locations close to (but not including) the fovea showed significant GCL thinning, whereas locations away from the fovea showed significantly increasing GCL thickening with increasing eccentricity. A number of studies demonstrating a reduced ganglion cell complex in AMD<sup>9-14,20,48,49</sup> have suggested that spatial changes in the GCL relate to outer retinal degeneration in AMD, with photoreceptor loss in the parafovea preceding foveal loss being well-established via histopathology.<sup>22</sup> This has also been supported by a number of psychophysical studies indicating rod photoreceptor deficits in the parafovea in early stages of AMD.<sup>23,50</sup> Thus, the increase in GCL thinning observed in our study may relate to the parafoveal susceptibility of the retina in AMD. The reasons behind an eccentricity dependent increase in GCL thickening, as observed in this study, however, are unclear. Histological study of mammalian retinae has demonstrated greater reduction of Müller cell volume compared to surface area in densely packed neuronal environments, suggesting that Müller cells fill into the available retinal space as enforced by its neuronal environment.<sup>51</sup> In our study, increased GCL thickening toward the periphery in AMD eyes could reflect

increased Müller cell hypertrophy and distension of its surface area toward retinal areas of greatest rod density (and subsequent post-receptor changes at the inner retina). These alterations in the outer retinal neuronal environment, alongside the sharp decline of ganglion cell density toward the peripheral macula,<sup>34</sup> could then translate into more “space” for the Müller cells’ surfaces to fill.

### Age-Correction of GCL Thickness can be Applied to Diseased Eyes

Establishing age and sex-matched control cohorts can prove difficult for studies of age-related diseases, such as AMD, due to a higher incidence of ocular disease in the elderly. To overcome this, for example, studies regarding visual field data have used age-correction functions to account for heterogeneous and under-sampled cohorts.<sup>25</sup> Once these functions were modeled, they were also useful in enabling the prediction of a participant’s output equivalent age based on input visual field results.<sup>52</sup> Our group recently described similar methodology for age-correction functions for GCL thickness changes across the macula, in accordance with the previously described spatial clusters.<sup>26,27</sup> Consequently, in this study, we found these functions could be applied to a control and diseased cohort to correct all GCL thickness data to the equivalent of a 65-year-old eye.

We found that when comparing the age-matched, age-corrected, and age-corrected<sub>non-age-matched</sub> analyses to each other, there were no significant differences with regard to the proportion of locations flagged with significant changes, nor with the magnitude of changes. The overall consistency between the analyses suggests age-corrected analysis of GCL thickness data may be useful for future studies that lack age-homogeneity or sufficient sample size of normal or diseased cohorts. Similarly, age-correction functions could also be applied in reverse to enable prediction of an output equivalent age based on GCL thickness input.

### Limitations

This study was associated with some limitations. First, inner retinal analysis was limited to the GCL. Others have indicated inner retinal remodeling in AMD involves other retinal layers, including the inner plexiform layer<sup>53</sup> and retinal nerve fibre layer,<sup>14,49</sup> and, as such, development of extended grid based analysis of other retinal layers is currently underway. Second, the nature of OCT means the cellular components, which contributed to the increase or decrease in GCL thickness observed in each grid location, is unknown. Assessment of layer reflectivity or histological analysis is needed to explore this further. Finally, this study was cross-sectional in nature, which restricts speculation on the significance of GCL changes over time. Other studies, however, have shown associations between inner retinal changes and prognostic outer retinal features in AMD, such as photoreceptor integrity,<sup>12</sup> and, therefore, it is possible these changes also have an association with AMD progression.

### CONCLUSION

GCL thickness changed significantly and nonuniformly within the macula of intermediate AMD eyes, with thinning at clusters toward the fovea, and thickening at clusters toward the peripheral macula. Further characterization of

these changes and mechanisms are critical to improve diagnoses and monitoring of GCL-altering pathologies within a clinical context.

### Acknowledgments

The authors thank Judy Nam, Nikki Pham, Katherine Duong, Nicholas Tan, and Georgina Uttley for technical assistance.

Supported by the Australian Postgraduate PhD scholarship (MT). Guide Dogs NSW/ACT provides support for the Centre for Eye Health (the clinic of recruitment), top-up PhD scholarship (NY), and salary support (JT, BZ, MK, and LN-S). Supported, in part, by a research grant from the Rebecca Cooper Foundation (LN-S).

Disclosure: **M. Trinh**, None; **J. Tong**, None; **N. Yoshioka**, None; **B. Zangerl**, None; **M. Kalloniatis**, None; **L. Nivison-Smith**, None

### References

1. Wong WL, Su X, Li X, et al. Global prevalence of age-related macular degeneration and disease burden projection for 2020 and 2040: A systematic review and meta-analysis. *Lancet Glob Health*. 2014;2:e106–e116.
2. Bhagat PR, Deshpande KV, Natu B. Utility of ganglion cell complex analysis in early diagnosis and monitoring of glaucoma using a different spectral domain optical coherence tomography. *J Curr Glaucoma Pract*. 2014;8:101–106.
3. Pincelli Netto M, Castro Lima V, Pacheco MA, Unonius N, P.B. Gracitelli C, Santos Prata T. Macular inner retinal layer thinning in diabetic patients without retinopathy measured by spectral domain optical coherence tomography. *Med Hypothesis Discov Innov Ophthalmol*. 2018;7:133–139.
4. Griffith JF, Goldberg JL. Prevalence of comorbid retinal disease in patients with glaucoma at an academic medical center. *Clin Ophthalmol Auckl NZ*. 2015;9:1275–1284.
5. He M-S, Chang F-L, Lin H-Z, Wu J-L, Hsieh T-C, Lee Y-C. The association between diabetes and age-related macular degeneration among the elderly in Taiwan. *Diabetes Care*. 2018;41:2202–2211.
6. Medeiros NE, Curcio CA. Preservation of ganglion cell layer neurons in age-related macular degeneration. *Invest Ophthalmol Vis Sci*. 2001;42:795–803.
7. Sullivan RKP, WoldeMussie E, Pow DV. Dendritic and synaptic plasticity of neurons in the human age-related macular degeneration retina. *Invest Ophthalmol Vis Sci*. 2007;48:2782–2791.
8. Jones BW, Pfeiffer RL, Ferrell WD, Watt CB, Tucker J, Marc RE. Retinal remodeling and metabolic alterations in human AMD. *Front Cell Neurosci*. 2016;10:103.
9. Camacho P, Dutra-Medeiros M, Páris L. Ganglion cell complex in early and intermediate age-related macular degeneration: Evidence by SD-OCT manual segmentation. *Ophthalmologica*. 2017;238:31–43.
10. Muftuoglu IK, Ramkumar HL, Bartsch D-U, Meshi A, Gaber R, Freeman WR. Quantitative analysis of the inner retinal layer thicknesses in age-related macular degeneration using corrected optical coherence tomography segmentation. *Retina*. 2018;38:1478–1484.
11. Savastano MC, Minnella AM, Tamburrino A, Giovinco G, Ventre S, Falsini B. Differential vulnerability of retinal layers to early age-related macular degeneration: evidence by SD-OCT segmentation analysis. *Invest Ophthalmol Vis Sci*. 2014;55:560–566.
12. Borrelli E, Abdelfattah NS, Uji A, Nittala MG, Boyer DS, Sadda SR. Postreceptor neuronal loss in intermediate

- age-related macular degeneration. *Am J Ophthalmol*. 2017;181:1–11.
13. Yenice E, Şengün A, Soyugelen Demirok G, Turaçlı E. Ganglion cell complex thickness in nonexudative age-related macular degeneration. *Eye*. 2015;29:1076–1080.
  14. Zucchiatti I, Parodi MB, Pierro L, et al. Macular ganglion cell complex and retinal nerve fiber layer comparison in different stages of age-related macular degeneration. *Am J Ophthalmol*. 2015;160:602–607.e1.
  15. Lamin A, Oakley JD, Dubis AM, Russakoff DB, Sivaprasad S. Changes in volume of various retinal layers over time in early and intermediate age-related macular degeneration. *Eye*. 2019;33:428–434.
  16. Toto L, Borrelli E, Di Antonio L, Carpineto P, Mastropasqua R. Retinal vascular plexuses' changes in dry age-related macular degeneration, evaluated by means of optical coherence tomography angiography. *Retina*. 2016;36:1566–1572.
  17. Yu J, Gu R, Zong Y, et al. Relationship between retinal perfusion and retinal thickness in healthy subjects: An optical coherence tomography angiography study. *Invest Ophthalmol Vis Sci*. 2016;57:OCT204–OCT210.
  18. Trinh M, Kalloniatis M, Nivison-Smith L. Vascular changes in intermediate age-related macular degeneration quantified using optical coherence tomography angiography. *Transl Vis Sci Technol*. 2019;8:20.
  19. Maynard ML, Zele AJ, Kwan AS, Feigl B. Intrinsically photosensitive retinal ganglion cell function, sleep efficiency and depression in advanced age-related macular degeneration. *Invest Ophthalmol Vis Sci*. 2017;58:990–996.
  20. Lee EK, Yu HG. Ganglion cell–Inner plexiform layer and peripapillary retinal nerve fiber layer thicknesses in age-related macular degeneration. *Invest Ophthalmol Vis Sci*. 2015;56:3976–3983.
  21. Brandl C, Brückmayer C, Günther F, et al. Retinal layer thicknesses in early age-related macular degeneration: Results from the German AugUR Study. *Invest Ophthalmol Vis Sci*. 2019;60:1581–1594.
  22. Curcio CA, Medeiros NE, Millican CL. Photoreceptor loss in age-related macular degeneration. *Invest Ophthalmol Vis Sci*. 1996;37:1236–1249.
  23. Owsley C, Jackson GR, Cideciyan AV, et al. Psychophysical evidence for rod vulnerability in age-related macular degeneration. *Invest Ophthalmol Vis Sci*. 2000;41:267–273.
  24. Clemons TE, Milton RC, Klein R, Seddon JM, Ferris FL; Age-Related Eye Disease Study Research Group. Risk factors for the incidence of Advanced Age-Related Macular Degeneration in the Age-Related Eye Disease Study (AREDS) AREDS report no. 19. *Ophthalmology*. 2005;112:533–539.
  25. Olsson J, Asman P, Heijl A. A perimetric learner's index. *Acta Ophthalmol Scand*. 1997;75:665–668.
  26. Tong J, Phu J, Khuu SK, et al. Development of a spatial model of age-related change in the macular ganglion cell layer to predict function from structural changes. *Am J Ophthalmol*. 2019;208:166–177.
  27. Yoshioka N, Zangerl B, Nivison-Smith L, et al. Pattern recognition analysis of age-related retinal ganglion cell signatures in the human eye. *Invest Ophthalmol Vis Sci*. 2017;58:3086–3099.
  28. Choi AYJ, Nivison-Smith L, Phu J, et al. Contrast sensitivity isocontours of the central visual field. *Sci Rep*. 2019;9:1–14.
  29. Phu J, Khuu SK, Nivison-Smith L, et al. Pattern recognition analysis reveals unique contrast sensitivity isocontours using static perimetry thresholds across the visual field. *Invest Ophthalmol Vis Sci*. 2017;58:4863–4876.
  30. Phu J, Khuu SK, Bui BV, Kalloniatis M. Application of pattern recognition analysis to optimize Hemifield asymmetry patterns for early detection of glaucoma. *Transl Vis Sci Technol*. 2018;7:3.
  31. Jamous KF, Kalloniatis M, Hennessy MP, Agar A, Hayen A, Zangerl B. Clinical model assisting with the collaborative care of glaucoma patients and suspects. *Clin Experiment Ophthalmol*. 2015;43:308–319.
  32. Lee H-J, Kim M-S, Jo Y-J, Kim J-Y. Macular ganglion cell complex and retinal nerve fiber layer comparison in different stages of age-related macular degeneration. *Am J Ophthalmol*. 2016;161:214.
  33. Ferris FL, Wilkinson CP, Bird A, et al. Clinical classification of age-related macular degeneration. *Ophthalmology*. 2013;120:844–851.
  34. Curcio CA, Allen KA. Topography of ganglion cells in human retina. *J Comp Neurol*. 1990;300:5–25.
  35. Yoshioka N, Zangerl B, Phu J, et al. Consistency of structure-function correlation between spatially scaled visual field stimuli and in vivo OCT ganglion cell counts. *Invest Ophthalmol Vis Sci*. 2018;59:1693–1703.
  36. Klein R, Meuer SM, Myers CE, et al. Harmonizing the classification of age-related macular degeneration in the three continent AMD Consortium. *Ophthalmic Epidemiol*. 2014;21:14–23.
  37. Eriksson U, Alm A, Larsson E. Is quantitative spectral-domain superior to time-domain optical coherence tomography (OCT) in eyes with age-related macular degeneration? *Acta Ophthalmol (Copenh)*. 2012;90:620–627.
  38. Kim SY, Sadda S, Pearlman J, et al. Morphometric analysis of the macula in eyes with disciform age-related macular degeneration. *Retina*. 2002;22:471–477.
  39. Schlanitz FG, Baumann B, Kundi M, et al. Drusen volume development over time and its relevance to the course of age-related macular degeneration. *Br J Ophthalmol*. 2017;101:198–203.
  40. Chua J, Nivison-Smith L, Fletcher EL, Trenholm S, Awatramani GB, Kalloniatis M. Early remodeling of Müller cells in the *rd/rd* mouse model of retinal dystrophy: Müller Cells in *rd/rd* mouse retina. *J Comp Neurol*. 2013;521:2439–2453.
  41. Cheng D, Wang Y, Huang S, et al. Macular inner retinal layer thickening and outer retinal layer damage correlate with visual acuity during remission in Behcet's disease. *Invest Ophthalmol Vis Sci*. 2016;57:5470–5478.
  42. Nagasaka Y, Ito Y, Ueno S, Terasaki H. Increased aqueous flare is associated with thickening of inner retinal layers in eyes with retinitis pigmentosa. *Sci Rep*. 2016;6:33921.
  43. DiLoreto DA, Martzen MR, del Cerro C, Coleman PD, del Cerro M. Müller cell changes precede photoreceptor cell degeneration in the age-related retinal degeneration of the Fischer 344 rat. *Brain Res*. 1995;698:1–14.
  44. Brynkskov T, Laugesen CS, Floyd AK, Sørensen TL. Thickening of inner retinal layers in the parafovea after bariatric surgery in patients with type 2 diabetes. *Acta Ophthalmol (Copenh)*. 2016;94:668–674.
  45. Pilotto E, Benetti E, Convento E, et al. Microperimetry, fundus autofluorescence, and retinal layer changes in progressing geographic atrophy. *Can J Ophthalmol J Can Ophthalmol*. 2013;48:386–393.
  46. Ozaki E, Campbell M, Kiang A-S, Humphries M, Doyle SL, Humphries P. Inflammation in age-related macular degeneration. *Adv Exp Med Biol*. 2014;801:229–235.
  47. Sadigh S, Cideciyan AV, Sumaroka A, et al. Abnormal thickening as well as thinning of the photoreceptor layer in intermediate age-related macular degeneration. *Invest Ophthalmol Vis Sci*. 2013;54:1603–1612.
  48. Gomez ML, Mojana F, Bartsch D-U, Freeman WR. Imaging of long-term retinal damage after resolved cotton wool spots. *Ophthalmology*. 2009;116:2407–2414.
  49. Ramkumar HL, Nguyen B, Bartsch D-U, et al. Reduced ganglion cell volume on optical coherence tomography in

- patients with geographic atrophy. *Retina*. 2018;38:2159–2167.
50. Brown B, Brabyn L, Welch L, Haegerstrom-Portnoy G, Colenbrander A. Contribution of vision variables to mobility in age-related maculopathy patients. *J Optom*. 1986;63:733–739.
  51. Chao TI, Grosche J, Friedrich KJ, et al. Comparative studies on mammalian Müller (retinal glial) cells. *J Neurocytol*. 1997;26:439–454.
  52. Bengtsson B, Heijl A. Inter-subject variability and normal limits of the SITA Standard, SITA Fast, and the Humphrey Full Threshold computerized perimetry strategies, SITA STATPAC. *Acta Ophthalmol Scand*. 1999;77:125–129.
  53. Muftuoglu IK, Lin T, Freeman WR. Inner retinal thickening in newly diagnosed choroidal neovascularization. *Graefes Arch Clin Exp Ophthalmol*. 2018;256:2035–2040.